Hindawi
Mathematical Problems in Engineering
Volume 2020, Article ID 4785839, 10 pages
https://doi.org/10.1155/2020/4785839

Research Article

Study on Distribution Characteristics of Damage Range along Smooth Blasting Hole Based on PPV

Qiang Pan, Jichun Zhang, and Shuangying Zheng

School of Civil Engineering, Southwest Jiaotong University, Chengdu, Sichuan 610031, China

Correspondence should be addressed to Shuangying Zheng; zsy2012@swjtu.edu.cn

Received 16 December 2019; Revised 21 March 2020; Accepted 2 April 2020; Published 25 April 2020

Academic Editor: Jan Vorel

The damage range of surrounding rock has an important influence on optimization of blasting parameters. This study, based on the vibration attenuation law near the blasting source and the characteristics of the load acting on the wall of the smooth blasting hole, derives the distribution formulas of the damage range along the borehole during the expansion and quasistatic processes of detonation gas, respectively. More importantly, the quantitative relationship between the damage range and the charge weight of the single borehole is established. The experimental data are used to verify the correctness of the theoretical formulas. The results show that the damage range during the expansion process of detonation gas presents a continuous saddle-shaped distribution along the borehole and the maximum damage range is near the charge segment. The damage range during the quasistatic process of detonation gas is uniformly distributed along the borehole and can be more conservatively used to the practical prediction after corrected. The theoretical formulas are applicable to the perimeter hole with the radial and axial decoupled charge structure, which can provide a theoretical support for controlling the damage range of surrounding rock according to the charge weight.

1. Introduction

Explosion stress in rock mass travels as a wave. For a particle, it is shown in the form of vibration. Blasting damage of rock mass is related to peak particle velocity (PPV), so PPV is often used to predict or evaluate blasting damage [1, 2]. Obviously, it is feasible to obtain the damage range from PPV and necessary to communicate the relationship between them. The characteristics of load acting on the borehole wall at the charge segment and the air segment are not exactly the same because the decouple charge structure is often used in the smooth blasting hole and detonation gas experiences the adiabatic expansion and the quasistatic processes successively. Thus, building a relationship among PPV, pressure on the borehole wall, and the damage range and exploring the distribution characteristics of the damage range along the borehole are of theoretical significance to reveal the mechanism of smooth blasting. Moreover, the amount of doing work to rock mass is directly determined by the charge weight of the borehole. From the perspective of energy, PPV is closely related to the charge weight whether near or far from the blasting source. Therefore, it is easy to control blasting damage in the field through building a relationship among PPV, the charge weight, and the damage range.

The vibration attenuation law far from the blasting source is applied to calculate vibration near the blasting source, in which the error is quite large [3]. It is shown that there are significant differences between vibration characteristics near the blasting source and those far from the blasting source. Besides, the vibration test near the blasting source needs high requirements for instruments and has difficulties in operation. Thus, the research results of vibration near the blasting source have been quite a few. Under the assumptions of detonating instantaneously and ignoring the direction of PPV caused by per unit charge, Holmberg and Persson [4] superposed the effect of per unit charge to calculate PPV near the blasting source of the cylindrical charge. Hustrulid and Lu [5] pointed out the mathematical errors in the Holmberg–Persson method and established the attenuation formula of PPV near the blasting source based on the subwave theory and the Heelan solution of the stress

wave field. Fu et al. [6] installed the sensors in the vault behind the tunnel face and right above and on the side of the middle pilot tunnel and then tested the vibration laws near the blasting source. Zhang et al. [7] applied the scaled distance to the vibration partitions in tunnel blasting based on the slope of the velocity curve and used the BP wavelet neural network to predict PPV near the blasting source. Xie et al. [8], based on the linear superposition theory, built a calculation model of PPV near the blasting source. Although the abovementioned studies enriched the blasting vibration theory to some extent, the differences of rock vibration at the charge segment and the air segment in the smooth blasting hole have not been clarified and the relationship between the damage range and PPV has not been communicated from the mechanism. Studying the damage range based on PPV is of importance to control the blasting damage and the charge weight because vibration near the blasting source determines the damage near the borehole directly.

Many scholars, based on PPV, focused on the study of the blasting damage threshold [9–12] and prediction of the blasting damage range [13–19]. Meanwhile, such methods as the SDOF method [20], the borehole extensometer measurement [21], the borehole TV observation [21], the plastic zone observation [22], the maximum plastic strain identification [22], and the effective strain identification [23] are combined to verify and complement each other. In addition, Hu et al. [24] studied the distribution characteristics of PPV near the blasting source and the correspondence between PPV and the damage degree. The PPV threshold of rock damage was determined. Dey and Murthy [1, 25] presented the PPV levels for crack initiation and widening and the PPV threshold for different degrees of overbreak or rock damage. Meanwhile, the vibration formula by Holmberg–Persson was extended and a formula evaluating the damage range was presented. Although the abovementioned studies preliminarily communicated the relationship between the damage range and PPV to some extent and enriched the blasting damage theory, there are still some further improvements. Firstly, the empirical formulas still need theoretical support and the numerical method and the field test also need theoretical guidance. Secondly, the distribution differences of blasting vibration and damage along the smooth blasting hole are not considered. Thirdly, the relationship between the damage range and the charge weight under axial interval charge is not involved. Therefore, it is necessary to theoretically study the distribution characteristics of the damage range along the smooth blasting hole and the relationship between the damage range and the charge weight so as to provide theoretical guidance for experiment and construction.

In this paper, based on the vibration attenuation law near the blasting source and the characteristics of the load acting on the wall of the smooth blasting hole, the relationship between PPV and the damage range is communicated in theory. Then, the formulas of the distribution characteristics of the damage range along the borehole are respectively derived during the expansion and quasistatic processes of detonation gas, The differences of the damage range at the charge segment and the air segment are revealed and the relationship between the damage range and the charge weight is communicated by the volumetric decoupling coefficient to predict the damage range. Therefore, this study can contribute to optimizing the blasting parameters reasonably and controlling the blasting damage effectively.

2. PPV Threshold of Blasting Damage

In the application of the damage criterion, the determination of the PPV threshold directly affects the accuracy in the prediction of the damage range. At present, the PPV threshold, determined by the P-wave velocity and the critical tensile strain based on the one-dimensional stress wave theory, has been widely used. Because rock mass around a borehole is generally in a state of the three-dimensional stress, the PPV threshold calculated by the one-dimensional stress wave theory has some errors. In addition, the PPV threshold is greatly influenced by characteristics of blasting load and properties of rock mass, so it is very difficult to obtain a precise value. Many scholars have usually adopted macroscopic investigation, field tests, numerical analysis, and so on to study the PPV threshold so far. According to the survey of the new cracks in rock mass and the comparison of acoustic wave before and after blasting, Bauer and Calder [26] suggested the blasting damage criterion based on PPV, as shown in Table 1. Holmberg and Persson [4] thought the safety upper limit of PPV in hard bedrock is 70~100 cm/s. Mojtabai and Beattie [27], based on the uniaxial compressive strength and the RQD of rock mass, gave the PPV threshold, respectively, under different damage zones. Hu et al. [24] gave the PPV threshold of 60~70 cm/s by the numerical analysis and field tests. There are great differences in the selection of the threshold due to different properties of rock mass and different definitions and standards of damage. In general, the better the integrity of rock mass is, the larger the PPV threshold is. The range of the PPV threshold in common rock mass is 25~60 cm/s. In engineering, the PPV threshold is controlled by the lower limit of the control standard for security reasons.

3. Theoretical Derivation and Analysis

Based on the attenuation formula of PPV near the blasting source [28] and taking the PPV threshold of blasting damage as $[v]$, the relationship between the damage range, r_s, and $[v]$ can be obtained as follows:

$$r_s = \left(\frac{kp_d}{\rho_r C_p [v]}\right)^{1/\beta} r_b, \tag{1}$$

where k is the coefficient related to the quantity of the boreholes during one-kick detonation (near the blasting source, $k = 1$; far from the blasting source, k is the quantity of the boreholes during detonation at the same layer.), p_d is the peak pressure on the borehole wall, ρ_r is the density of rock mass, C_p is the average P-wave velocity of rock mass, β is the attenuation index which is related to rock mass, and r_b is the radius of the borehole.

Table 1: Rock damage effect under different PPV.

PPV (cm/s)	Rock damage effect
<25	Intact rock without crack
25~63.5	Producing a slight tensile crack
63.5~254	Producing a serious tensile crack and some radial cracks
>254	Completely fractured rock

The damage range in equation (1) is the distance from the boundary of the damage zone to the center of the borehole, but not the net distance to the borehole wall, as shown in Figure 1.

The transmission of stress wave is independent and symmetric near the blasting source before encountering the interference. Therefore, the vibration on the side of surrounding rock is the same as that in the smooth blasting layer. In addition, the PPV values appear near the initial point of vibration time-history, that is, they have already appeared before reaching the free surface. The vibration generated by reflection of free surface to the area near the blasting source is very small, which only affects the vibration characteristics of the later time-history after superposition but hardly affects the PPV values near the blasting source, especially the PPV values on the side of surrounding rock. Therefore, the PPV values near the blasting source are almost independent of the minimum burden. In conclusion, the abovementioned formulas can be applied to the smooth blasting hole.

The larger radial and axial decoupling coefficients are often used in the smooth blasting hole in order to weaken the impact effect on the borehole wall, so the initial expansion pressure of detonation gas, p_m, produced in each charge segment is the detonation pressure on the detonation wave front, not the average detonation pressure.

The initial dynamic pressure on the borehole wall, p_d, can be obtained by the adiabatic expansion law of detonation gas [29] and the pressure enhancement coefficient, n, when detonation gas collides with the borehole wall. For the strong impact, n is taken from 8 to 11. For the weak impact, n is taken from 2 to 8. In general, near the charge segment with a larger diameter, the action of detonation gas on the borehole wall belongs to the strong impact, while at the air interval segment or near the charge segment with a smaller diameter, it belongs to the weak impact.

The initial detonation gas expands radially and axially until it fills the whole borehole, which is known as the expansion process of detonation gas. The dynamic pressure is formed by the collisions between detonation gas and the borehole wall. After detonation gas fills the whole borehole, the pressure decreases slowly and action time is longer, which is called the quasistatic process of detonation gas. Quasistatic pressure is exerted on the borehole wall during this process. In addition, the radial expansion length of detonation gas after explosion of each charge segment is much smaller than the axial expansion length, which makes the difference of the pressure at the charge segment and the air segment, resulting in the differential damage range. To reveal the difference and predict the damage range, this study analyzes the damage distribution characteristics under the two action processes, respectively.

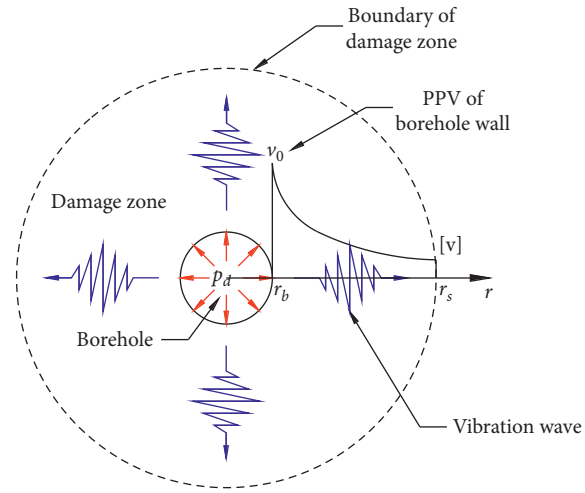

Figure 1: Damage range of the borehole based on the attenuation law of PPV.

3.1. Expansion Process of Detonation Gas. During the expansion process of detonation gas, the change laws of pressure on the borehole wall along the axial direction and the distribution characteristics of the damage range along the axial direction are studied. To emphasize the key and facilitate the analysis, the following assumptions are made:

(1) The initial volume of detonation gas is the same as the volume of the charge segment.

(2) The charge segments are distributed at the regular intervals along the borehole and detonation gas expands around the blasting source uniformly.

(3) The initial detonation gas produced by per charge segment expands to the air segment center finally and is not pressurized while colliding axially. It is pressurized by the collision only when expanding to the borehole wall laterally.

(4) Pressure on the borehole wall is equal everywhere and the pressure enhancement coefficient is constant within the range of the axial length when the initial detonation gas expands to the borehole wall exactly and laterally. However, during the subsequent expansion process, the pressure enhancement coefficient decreases linearly along the borehole.

Three charge segments with Φ 32 mm of emulsion explosive used to cut into the short cartridges in the field are taken as an example to illustrate the expansion process of detonation gas, as shown in Figure 2, where the center of the charge segment is the original point of expansion (0 point), l is the unilateral expansion distance along the borehole, s is the center distance of two charge segments, l_0 is the length of per charge segment, l_k is the expansion distance under the critical pressure, d_b is the diameter of the borehole, and d_c is the diameter of the charge.

In the whole borehole, the expansion process of detonation gas is generally divided into three stages. The

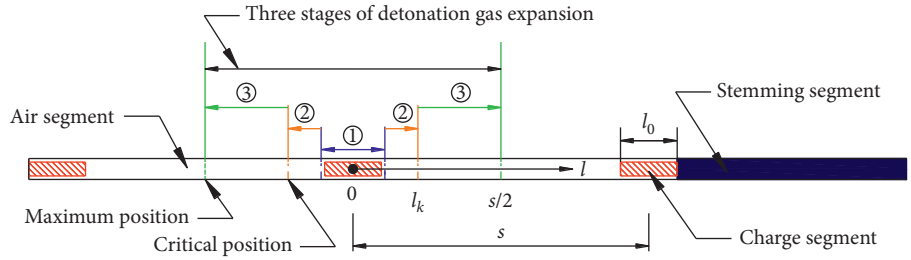

Figure 2: Expansion process of detonation gas in the smooth blasting hole.

expansion laws of detonation gas and the distribution characteristics of the damage range are analyzed as follows:

The first stage is that detonation gas expands laterally to the borehole wall, as shown in ① of Figure 2. The unilateral expansion range along the borehole is $(l_0/2) < l \le ((l_0 + d_b - d_c)/2)$.

The distribution formula of the damage range along the borehole is derived as follows:

$$r_s = \left(\frac{k p_m (d_c/d_b)^6 (l_0/(l_0 + d_b - d_c))^3 n_1}{(\rho_r C_p [v])} \right)^{1/\beta} r_b. \quad (2)$$

The second stage is that detonation gas expands to the position under the critical pressure ($p_k = 200$ MPa), as shown in ② of Figure 2. The unilateral expansion range along the borehole is $((l_0 + d_b - d_c)/2) < l \le l_k$.

The distribution formula of the damage range along the borehole is derived as follows:

$$r_s = \left(\frac{k p_m (d_c/d_b)^6 (l_0/(2l))^3 n_2}{(\rho_r C_p [v])} \right)^{1/\beta} r_b. \quad (3)$$

The third stage is that detonation gas expands to the air segment center, as shown in ③ of Figure 2. The unilateral expansion range along the borehole is $l_k < l \le (s/2)$.

The distribution formula of the damage range along the borehole is derived as follows:

$$r_s = \left(\frac{k p_k (p_m/p_k)^{\gamma/3} (d_c/d_b)^{2\gamma} (l_0/(2l))^{\gamma} n_3}{(\rho_r C_p [v])} \right)^{1/\beta} r_b. \quad (4)$$

where γ is the isentropic index and can be taken as 4/3.

The ratio of the maximum and the minimum value of the damage range is calculated as follows:

$$\delta = \frac{r_{s(\max)}}{r_{s(\min)}} = \left(\frac{p_m}{p_k} \right)^{(3-\gamma)/(3\beta)} \left(\frac{d_c}{d_b} \right)^{(6-2\gamma)/\beta} \left(\frac{l_0}{l_0 + d_b - d_c} \right)^{3/\beta} \cdot \left(\frac{l_0}{s} \right)^{-\gamma/\beta} \left(\frac{n_1}{n_3} \right)^{1/\beta}. \quad (5)$$

In particular, if the special cartridges of smooth blasting are used, pressure produced by the lateral expansion of detonation gas exactly to the borehole wall will be less than the critical pressure. Thus, the abovementioned first stage will experience two action processes of high pressure and low pressure successively. In the second stage, detonation gas expands to the air segment center.

3.2. Quasistatic Process of Detonation Gas. In fact, the quasistatic action is carried out on the basis of detonation gas expansion. In order to analyze the single quasistatic action process, it is thought that detonation gas fills the borehole instantaneously during the quasistatic process and the damage caused by detonation gas expansion is not considered. Although the quasistatic pressure is relatively smaller and changes slowly, damage to surrounding rock cannot be ignored because of the longer action time. Meanwhile, in smooth blasting, damage caused by the quasistatic action also affects the directional fracture controlled by the quasistatic action. In addition, the special cartridge for smooth blasting should be in principle adopted in the borehole, but due to the limited site condition, Φ 32 mm ordinary emulsion cartridge is used to cut into many short cartridges from 7 cm to 10 cm for interval charge, which makes surrounding rock near the charge segment produce the local fracture and the blasting cracks easily, as shown in Figure 3. In smooth blasting, not only the local effect near the charge segment is focused on but also the overall effect of the whole borehole is concerned. More importantly, the quantitative relationship between the damage range and the charge weight of the borehole is established so as to control damage of surrounding rock through changing the charge weight. Thus, the volumetric decoupling coefficient which reflects the overall effect is adopted to make an integral analysis on the quasistatic process.

The quasistatic pressure, p_j, of detonation gas expanding to fill the borehole and the average equivalent dynamic pressure, p_d, are as follows:

$$p_j = p_k \left(\frac{p_m}{p_k} \right)^{\gamma/3} \left(\frac{1}{K_V} \right)^{\gamma}, \quad (6)$$

$$p_d = p_k \left(\frac{p_m}{p_k} \right)^{\gamma/3} \left(\frac{1}{K_V} \right)^{\gamma} n_0, \quad (7)$$

where K_V is the volumetric decoupling coefficient and n_0 is the pressure enhancement coefficient of the borehole wall under the action of quasistatic gas, whose value is relatively smaller.

The blasting damage range of rock mass under the action of quasistatic gas can be derived from the definition formula of K_V, equation (1) and (7), as follows:

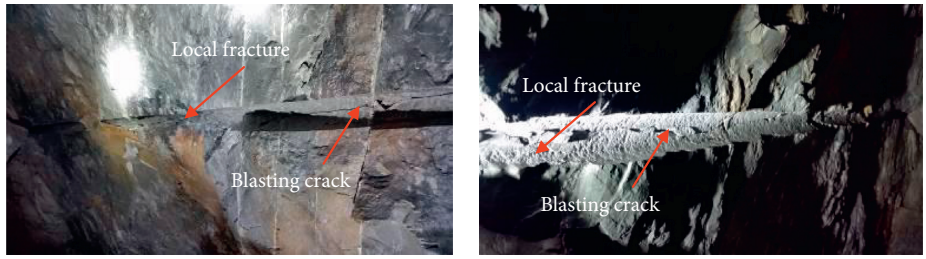

(a) (b)

Figure 3: Local fracture and blasting cracks near the charge segment in the smooth blasting hole. (a) Borehole of the vault. (b) Borehole of the side wall.

$$r_s = \left(\frac{k p_k n_0}{\rho_r C_p [v]} \left(\frac{p_m}{p_k} \right)^{\gamma/3} \left(\frac{1}{\rho V_b} \right)^{\gamma} Q^{\gamma} \right)^{1/\beta} r_b, \quad (8)$$

where V_b is the borehole volume, Q is the charge weight of the borehole, and ρ is the explosive density.

In equation (8), the quantitative relationship between the damage range and the charge weight of the borehole under the action of quasistatic gas is established. It reflects the overall effect of the quasistatic process when detonation gas fills the whole borehole, not the local effect near the charge segment. Therefore, it can be applied to the perimeter hole with the radial and axial decouple charge structure.

In conclusion, the distribution characteristics of the damage range along the borehole during the expansion and quasistatic processes of detonation gas are drawn in Figure 4.

During the expansion process of detonation gas, the damage range presents a continuous saddle-shaped distribution along the borehole, as shown in Figure 4. The maximum damage range is near per charge segment. The minimum damage range is near per air segment center. Therefore, the dynamic action of the isentropic adiabatic expansion of detonation gas is revealed fully. The damage range is a function of both time and space and is closely related to the load characteristics along the borehole.

The damage range along the borehole is uniformly distributed during the quasistatic process of detonation gas, as shown in Figure 4, which fully reveals the quasistatic action after detonation gas fills the whole borehole. In addition, the damage range with the uniform distribution is slightly larger than the minimum damage range during the expansion process of detonation gas, mainly due to the assumption that the charge segments at the bottom and top of the borehole expand bilaterally and each charge segment expands ultimately to the air segment center.

In fact, there are differences in the damage range of surrounding rock when a charge segment is in different positions of the borehole, such as at the bottom, middle, and top. It is mainly because that detonation gas produced by the charge segment in different positions is constrained differently during the axial expansion, which causes different action strength to the borehole wall.

For safety reasons, the most unfavorable conditions are considered, namely, the blasting damage range is uniformly distributed along the borehole and is equal to the maximum damage range near the charge segment. The equation that

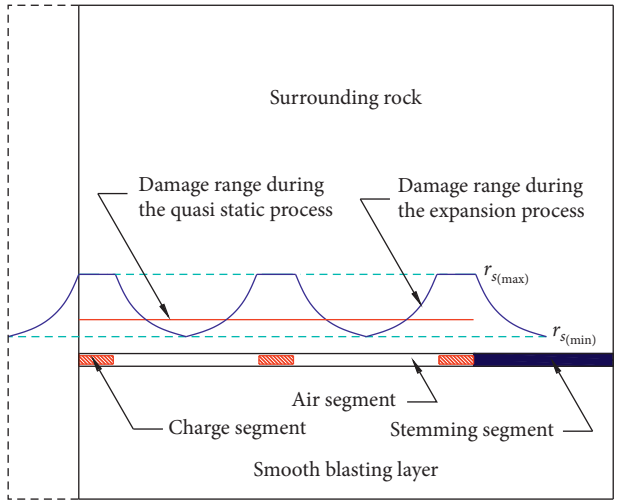

Figure 4: Distribution characteristics of the damage range along the smooth blasting hole in surrounding rock.

the damage range under the quasistatic action multiplies by the correction factor, δ, can be used to obtain the corrected damage range, namely,

$$r_x = \delta \left(\frac{k p_k n_0}{\rho_r C_p [v]} \left(\frac{p_m}{p_k} \right)^{\gamma/3} \left(\frac{1}{\rho V_b} \right)^{\gamma} Q^{\gamma} \right)^{1/\beta} r_b, \quad (9)$$

where δ is the ratio of the maximum and the minimum values of the damage range during the expansion process of detonation gas.

4. Verification of Model Experiment

4.1. Experiment Scheme. Fine stone concrete is used to pour a rectangle model with 600 cm in length, 150 cm in width, and 90 cm in height. The curing time is more than 28 days under the natural conditions. Meanwhile, the cubic standard samples with a length of 150 mm are made. After the curing, the physical and mechanical parameters of standard samples are tested, which are given in Table 2. Multiple-row boreholes with 40 mm in diameter and 80 cm in depth are laid in the concrete model along the length direction. There are 3 or 4 boreholes in a row. A guide hole is respectively arranged close to each side of the boundary. According to the previous model experiments, the blasting parameters are determined,

Table 2: Physical and mechanical parameters of fine stone concrete in the model experiments.

Density (kg/m^3)	Elasticity modulus (GPa)	Poisson's ratio	P-wave velocity (m/s)	Uniaxial compressive strength (MPa)
2356	36.68	0.27	4457	37.2

Table 3: Borehole parameters and charge parameters for smooth blasting in the model experiments.

Borehole diameter (mm)	Borehole depth (cm)	Single charge length (cm)	Stemming length (cm)	Radial decoupling coefficient	Linear charge density (kg/m)
40	80	4	30	1.77	0.05

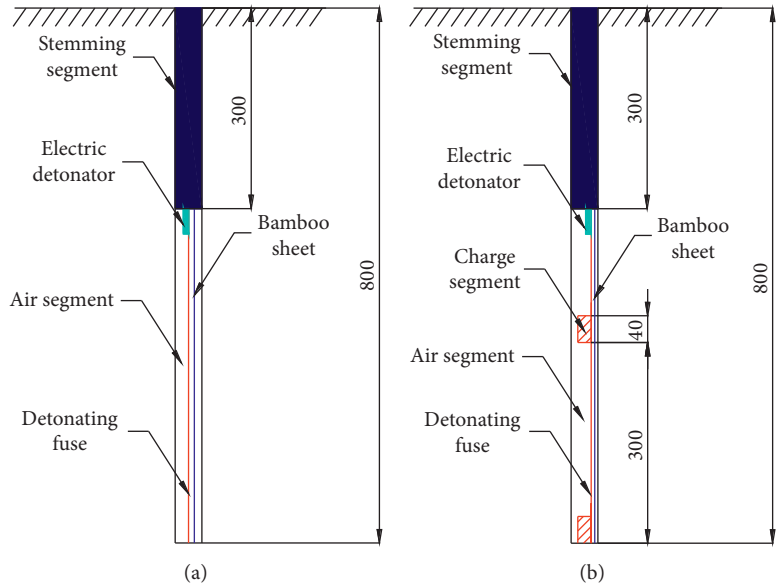

Figure 5: Charge structure of the smooth blasting hole at different locations (unit, mm). (a) Side borehole. (b) Middle borehole.

as shown in Table 3. Two blasting experiments with 50 cm borehole spacing and 40 cm and 60 cm minimum burdens are chosen to analyze.

In the model experiments, each borehole consists of two charge segments up and down for the axial interval charge. Detonating fuse is used to detonate in series. However, the boreholes near the boundary only adopt detonating fuse to detonate in order to reduce the boundary effect. The charge structures of the boreholes are shown in Figure 5. A row of horizontally dense holes with 10 cm spacing and 10 mm diameter are drilled on the boundary of the borehole connection line along the height direction. So, the boundary after blasting is flat for testing the P-wave velocity easily.

During the P-wave test process, test lines are densely laid near the charge segment along the direction perpendicular to the borehole, while test lines are, in turn, sparsely laid toward the air interval zones with 3~8 cm spacing. Test lines are densely laid with 5 cm spacing near the borehole along the direction parallel to the borehole, while test lines are sparsely laid far from the borehole with 10 cm spacing. The cross points of the vertical and horizontal test lines are used as the test points. The test lines and test points are laid, as shown in Figure 6. In order to ensure the centering of the transmitting probe and receiving probe, many auxiliary circles equal to the diameter of the probe at the cross points of the test lines are drawn so that the test probe just covers the drawn circles. Then, the RSM-SY5(T) acoustic detector is adopted for the test. The test probe should be tightly bonded with coupling agents and concrete. The test process is shown in Figure 7 and the test curves are drawn in Figure 8.

4.2. Verification and Analysis. Based on the equivalent strain principle of elastic damage theory and the assumption that material density and Poisson's ratio are constant before and after damage, the damage variable can be expressed as [30]

$$D = 1 - \frac{E}{E_0} = 1 - \left(\frac{c}{c_0}\right)^2, \tag{10}$$

where E_0 is the elastic modulus before blasting, c_0 is the P-wave velocity before blasting, E is the elastic modulus after blasting, and c is the P-wave velocity after blasting.

Since the P-wave velocity is easy to test and will not cause secondary damage to the material, the damage value can be calculated by equation (10) according to the measured P-wave velocity.

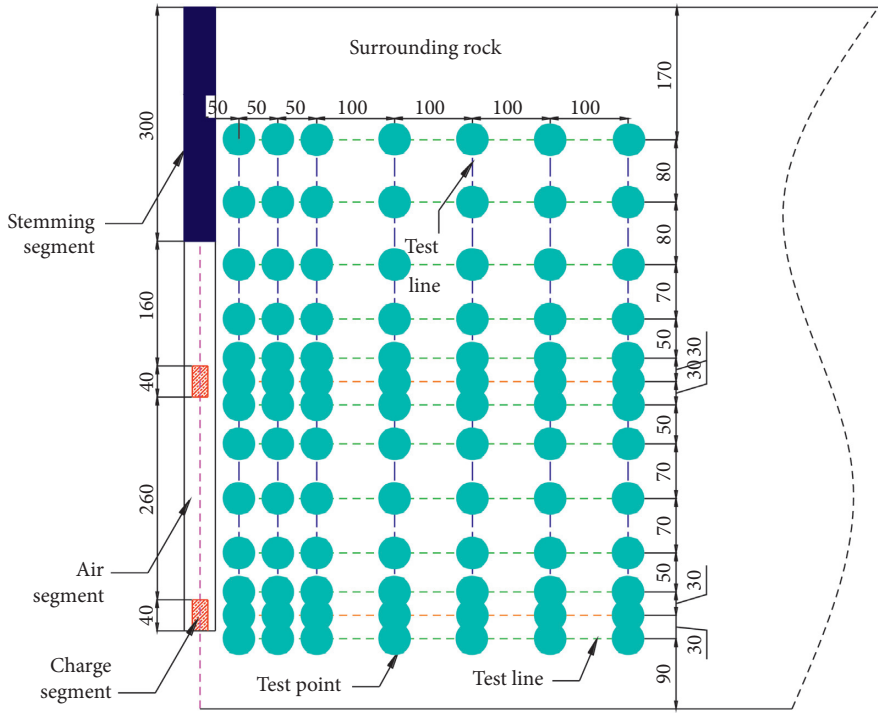

Figure 6: Layout of test lines and test points on the side of surrounding rock (unit, mm).

Figure 7: Test of P-wave velocity before and after blasting.

In consideration of the strength of fine stone concrete in the model experiments and the on-site rock mass condition, the widely used threshold of PPV proposed by Bauer and Calder can be adopted to the theoretical analysis, namely, 25 cm/s, for tunnel design and construction safety. Due to the significant differences of concrete and rock mass, the damage threshold of fine stone concrete is taken as 0.05 in the experimental data analysis. In addition, the damage value between the two test points perpendicular to the borehole can be obtained by linear interpolation. According to the blasting damage values under two different minimum burdens, the distribution curve of the damage range along the borehole is drawn, as shown in Figure 9.

Distribution characteristics of the measured damage range present a continuous saddle-shaped distribution along the borehole, as shown in Figure 9, which manifests that the maximum damage range is near the charge segment and the minimum damage range is usually near the stemming segment. When the stemming result is effective, only a small part of the stemming segment is compressed by detonation gas, while surrounding rock at the uncompressed stemming segment is hardly damaged by blasting. Macroscopic characteristics after blasting at different positions of the

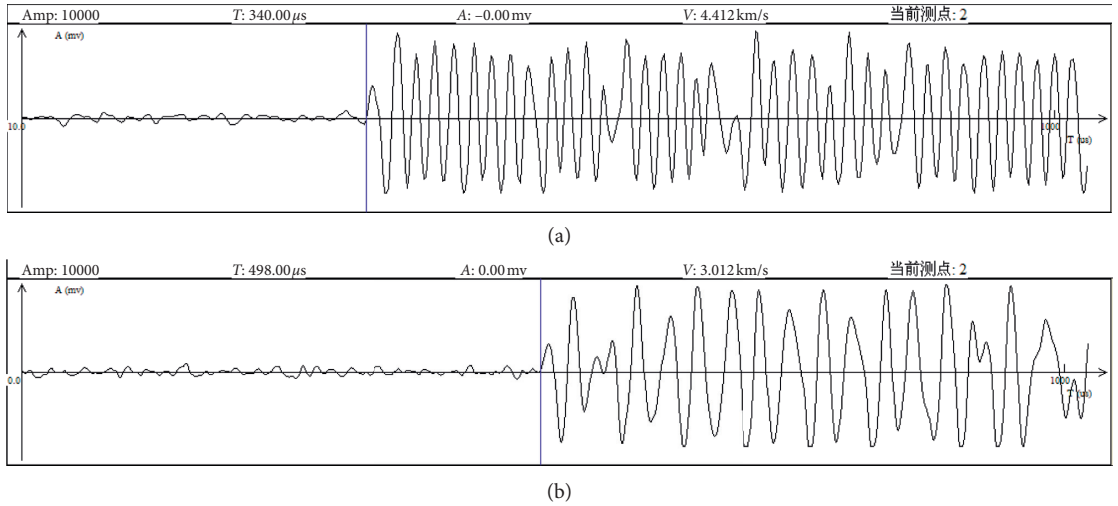

Figure 8: P-wave curves (a) before blasting and (b) after blasting.

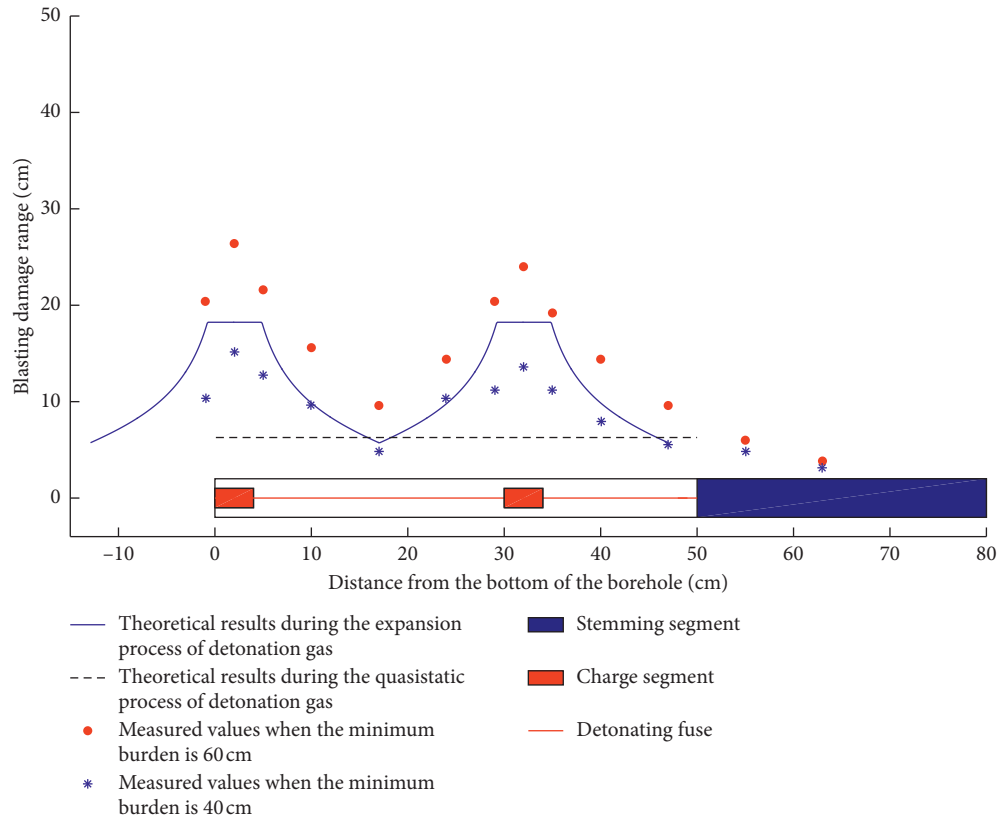

Figure 9: Measured values and distribution curves of the damage range along the borehole under different minimum burdens.

boreholes are shown in Figures 10 and 11. Due to the stronger impact effect near the charge segment, the damage range and degree are the largest. Therefore, the damage range near the charge segment can be used as a control basis for optimization of blasting parameters.

The damage range of surrounding rock increases with the increase of the minimum burden, as shown in the measured data of Figure 9. Due to the increase of the minimum burden, more blasting energy is transferred to the side of surrounding rock and the load time is prolonged. Therefore, the minimum burden should not be too large in practice; otherwise, it will affect the fragmentation effect and increase damage. If the minimum burden is too large, the linear charge density needs to be increased in order to achieve the fragmentation effect, which is bound to increase the damage range of surrounding rock.

The theoretical calculation results are basically consistent with the measured change law of the model experiments, as

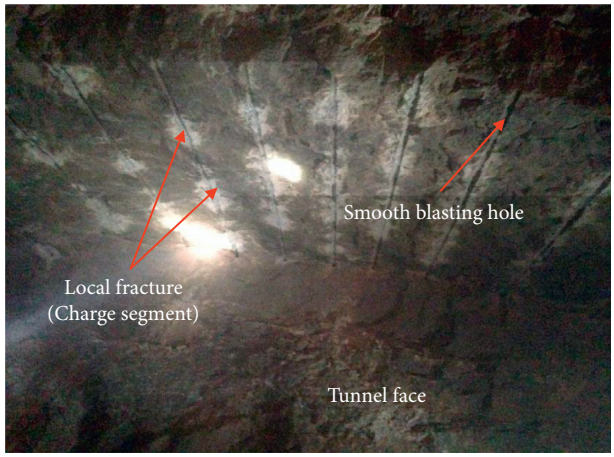

Figure 10: Macroscopic characteristics of surrounding rock along the borehole after the on-site smooth blasting.

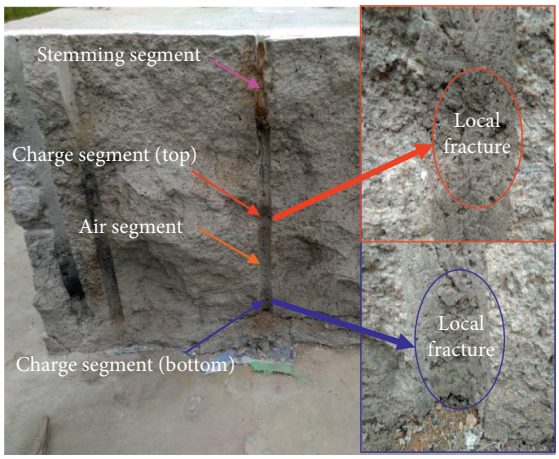

Figure 11: Macroscopic characteristics of surrounding rock along the borehole after smooth blasting in the model experiments.

shown in Figure 9, which can reflect the distribution characteristics of the damage range along the borehole and predict the damage range. However, there is a certain difference between the theoretical values and the measured values for the following main reasons. First, the time factor and the minimum burden are not taken into consideration in the theoretical formulas. Second, there is a certain difference between the assumption and the reality. Third, the measured values are the combined result of the two processes. Thus, the theoretical formulas can still provide theoretical support for the control of blasting damage.

This study assumes that all the charge segments have the same length. In fact, charge should be strengthened at the bottom of the borehole in order to overcome the rock clamping force and increase the utilization effect of the borehole. Therefore, the length of the larger damage range at the bottom of the borehole is also increased.

The theoretical formula established in this study based on PPV does not involve the influence of the minimum burden (thickness of the smooth blasting layer). However, in fact, the damage range is related to the minimum burden, that is, the minimum burden determines the quantity of energy transferred to surrounding rock and the duration of load.

5. Conclusion

Based on the vibration attenuation law near the blasting source and the characteristics of the load acting on the wall of the smooth blasting hole, the theoretical formulas of the damage range along the borehole are derived and verified by the measured values. The main conclusions are drawn as follows:

(1) During the expansion process of detonation gas, the damage range presents a continuous saddle-shaped distribution along the borehole and the maximum damage range is near the charge segment. During the quasistatic process of detonation gas, the damage range is uniformly distributed, whose value is slightly greater than the minimum value during the expansion process in theory.

(2) The damage range at the charge segment is different from that at the air segment during the process of expansion. The corrected damage range based on the differences can predict the damage range and optimize blasting parameters so as to control the damage range according to the charge weight.

(3) The derived theoretical formulas can reflect the distribution laws of the damage range along the borehole, which can be applied to the perimeter hole with radial and axial decoupled charge structure. In fact, the damage range increases with the increase of the minimum burden. However, the theoretical formulas based on PPV are difficult to reveal the influence of the minimum burden from the mechanism.

Further research might investigate the influence of the minimum burden and the theoretical superposition criterion of the damage range during the two processes.

Data Availability

The data used to support the findings of this study are available from the corresponding author upon request.

Conflicts of Interest

The authors declare that there are no conflicts of interest regarding the publication of this paper.

Acknowledgments

This work was supported by the National Natural Science Funds of China (50574076). The support and help during the model experiments from explosion and impact laboratory of Southwest University of Science and Technology, especially Associate Professor Chuanjin Pu and Dr. Dingjun Xiao, are sincerely appreciated.

References

[1] K. Dey and V. M. S. R. Murthy, "Determining blast damage envelope through vibration model and validation using seismic imaging," *Mining Technology*, vol. 120, no. 2, pp. 90–94, 2011.

[2] S. R Singh and R. D. Lamond, "Prediction and measurements of blast vibrations," *International Journal of Surface Mining, Reclamation and Environment*, vol. 7, no. 4, pp. 149–154, 1993.

[3] G. L. Yang, P. Rocque, P. Katsabanis, and W. F. Bawden, "Measurement and analysis of near-field blast vibration and damage," *Geotechnical and Geological Engineering*, vol. 12, no. 2, pp. 169–182, 1994.

[4] R. Holmberg and P. A. Persson, "Swedish approach to contour blasting,," in *Proceedings of the 4th Conference on Explosive and Blasting Technique*, pp. 113–127, New Orleans, LA, USA, February 1978.

[5] W. Hustrulid and W. B. Lu, "Some general design concepts regarding the control of blast induced damage during rock slope excavation,," in *Proceedings of the 7th International Symposium on Rock Fragmentation by Blasting*, pp. 595–604, Beijing, China, August 2002.

[6] H. X. Fu, Y. Zhao, J. S. Xie, and Y. B. Hou, "Study of blasting vibration test of area near tunnel source," *Chinese Journal of Rock Mechanics and Engineering*, vol. 30, no. 2, pp. 335–340, 2011.

[7] Z. C. Zhang, C. M. Lin, Z. B. Huang, B. Y. Ge, and L. Xu, "Prediction of blasting vibration of area near tunnel blasting source," *Explosion and Shock Waves*, vol. 34, no. 3, pp. 367–372, 2014.

[8] F. Xie, L. Han, D. S. Liu, and C. Li, "Study on the rule of blasting vibration of field near tunnel blasting source based on waveform superposition theory," *Journal of Vibration and Shock*, vol. 37, no. 2, pp. 182–188, 2018.

[9] F. S. Kendorski, C. V. Jude, and W. M. Duncan, "Effect of blasting on shortcrete drift linings," *Mining Engineering*, vol. 25, no. 12, pp. 38–41, 1973.

[10] P. K. Singh, "Blast vibration damage to underground coal mines from adjacent open-pit blasting," *International Journal of Rock Mechanics and Mining Sciences*, vol. 39, no. 8, pp. 959–973, 2002.

[11] H. B. Li, X. Xia, J. C. Li, J. Zhao, B. Liu, and Y. Q. Liu, "Rock damage control in bedrock blasting excavation for a nuclear power plant," *International Journal of Rock Mechanics and Mining Sciences*, vol. 48, no. 2, pp. 210–218, 2011.

[12] X. Xia, H. B. Li, J. C. Li, B. Liu, and C. Yu, "A case study on rock damage prediction and control method for underground tunnels subjected to adjacent excavation blasting," *Tunnelling and Underground Space Technology*, vol. 35, pp. 1–7, 2013.

[13] G. W. Ma, H. Hao, and Y. X. Zhou, "Modeling of wave propagation induced by underground explosion," *Computers and Geotechnics*, vol. 22, no. 3-4, pp. 283–303, 1998.

[14] M. Khandelwal and T. N. Singh, "Prediction of blast induced ground vibration and frequency in open cast mine: a neural network approach," *Journal of Sound and Vibration*, vol. 289, no. 4-5, pp. 711–725, 2006.

[15] C. Q. Wu and H. Hao, "Numerical prediction of rock mass damage due to accidental explosions in an underground ammunition storage chamber," *Shock Waves*, vol. 15, no. 1, pp. 43–54, 2006.

[16] J. Toraño, R. Rodríguez, I. Diego, J. M. Rivas, and M. D. Casal, "FEM models including randomness and its application to the blasting vibrations prediction," *Computers and Geotechnics*, vol. 33, no. 1, pp. 15–28, 2006.

[17] D. Saiang and E. Nordlund, "Numerical analyses of the influence of blast-induced damaged rock around shallow tunnels in brittle rock," *Rock Mechanics and Rock Engineering*, vol. 42, no. 3, pp. 421–448, 2009.

[18] H. R. Mohammadi Azizabadi, H. Mansouri, and O. Fouché, "Coupling of two methods, waveform superposition and numerical, to model blast vibration effect on slope stability in jointed rock masses," *Computers and Geotechnics*, vol. 61, pp. 42–49, 2014.

[19] I. Fullelove, I. Onederra, and E. Villaescusa, "Empirical approach to estimate rock mass damage from long-hole winze (LHW) blasting," *Mining Technology*, vol. 126, no. 1, pp. 34–43, 2017.

[20] M. Mohamed, A. M. Azrul, H. Roszilah, and N. R. Sudharshan, "Blast damage assessment of symmetrical box-shaped underground tunnel according to peak particle velocity (PPV) and single degree of freedom (SDOF) criteria," *Symmetry*, vol. 10, no. 5, p. 158, 2018.

[21] M. Ramulu, A. K. Chakraborty, and T. G. Sitharam, "Damage assessment of basaltic rock mass due to repeated blasting in a railway tunnelling project - a case study," *Tunnelling and Underground Space Technology*, vol. 24, no. 2, pp. 208–221, 2009.

[22] X. Y. Wei, Z. Y. Zhao, and J. Gu, "Numerical simulations of rock mass damage induced by underground explosion," *International Journal of Rock Mechanics and Mining Sciences*, vol. 46, no. 7, pp. 1206–1213, 2009.

[23] G. W. Ma, H. Hao, and F. Wang, "Simulations of explosion-induced damage to underground rock chambers," *Journal of Rock Mechanics and Geotechnical Engineering*, vol. 3, no. 1, pp. 19–29, 2011.

[24] Y. G. Hu, W. B. Lu, M. Chen, and P. Yan, "Determination of critical damage PPV near the blast hole of rock-mass," *Explosion and Shock Waves*, vol. 35, no. 4, pp. 547–554, 2015.

[25] K. Dey and V. M. S. R. Murthy, "Predicting overbreak from blast vibration monitoring in a lake tap tunnel-a success story," *Fragblast*, vol. 7, no. 3, pp. 149–166, 2003.

[26] A. Bauer and P. N. Calder, *Open Pit and Blast Seminar*, Mining Engineering Department, Ontario, Canada, 1978.

[27] N. Mojtabai and S. G. Beattie, "Empirical approach to prediction of damage in bench blasting," *Transaction of Institution of Mining and Metallurgy*, vol. 105, no. 1, pp. 75–80, 1996.

[28] W. B. Lu and W. Hustrulid, "Design approach for excavation blasting near contour of rock slope," *Chinese Journal of Rock Mechanics and Engineering*, vol. 22, no. 12, pp. 2052–2056, 2003.

[29] J. Henrych, *The Dynamics of Explosion and its Use*, Elsevier Scientific Publishing Company, Amsterdam, Netherlands, 1979.

[30] J. Lemaitre, *A Course on Damage Mechanics*, Springer, Berlin, Germany, 1992.